

# Specific Targeting of Proerythroblasts and Erythroleukemic Cells by the VP1u Region of Parvovirus B19

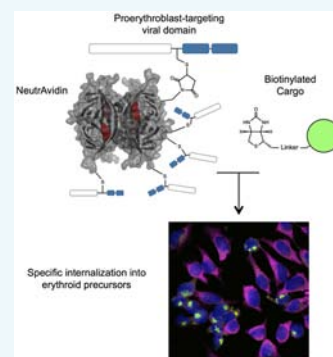
Remo Leisi,<sup>\*,†</sup> Marcus von Nordheim,<sup>†</sup> Christoph Kempf,<sup>†,‡</sup> and Carlos Ros<sup>\*,†,‡</sup>

<sup>†</sup>Department of Chemistry and Biochemistry, University of Bern, 3012 Bern, Switzerland

<sup>‡</sup>CSL Behring AG, 3014 Bern, Switzerland

## S Supporting Information

**ABSTRACT:** Viruses are evolutionarily developed cell-entering nanomachines, which are frequently used as gene or drug delivery systems. Parvovirus B19 (B19V) shows a remarkably restricted tropism for erythropoietin-dependent erythroid differentiation stages, and thus this virus provides an opportunity to deliver cargo to these intermediate differentiated cells. Here we report the construction of a delivery system from B19V subunits that maintains the highly selective cell-entry of the native virus and offers versatile cargo transport. To obtain this specific carrier, we conjugated the cell-targeting VP1u region of B19V to NeutrAvidin as a loading platform for biotinylated cargos. The VP1u–NeutrAvidin conjugate delivered fluorophores, DNA, and toxic payloads specifically to erythroid cells around the proerythroblast differentiation stage, including erythroleukemic cells. The VP1u–NeutrAvidin represents a unique cell surface marker which exclusively detects intermediate erythroid differentiation stages. Furthermore, the cell-entering property of this viral-based targeting system offers opportunities for erythroid-specific drug delivery or gene therapy.



## INTRODUCTION

Red blood cells are constantly being reproduced in the bone marrow by the differentiation of hematopoietic stem cells into erythrocytes. In the first days of erythropoiesis, hematopoietic stem cells differentiate into committed erythroid progenitors as burst-forming unit-erythroid (BFU-E) and then colony-forming unit-erythroid (CFU-E). The following erythroid differentiation into erythroblasts is dependent on the cytokine erythropoietin (EPO), including the stages CFU-E, proerythroblasts, and early basophilic erythroblasts.<sup>1–5</sup> The hallmark of these intermediate erythroid differentiation stages is EPO-dependence, increased cellular proliferation, and the beginning expression of erythroid-specific genes (e.g., globins, glycoporphins). The terminal erythroid differentiation is accompanied by the expression and accumulation of erythrocyte-specific proteins, the condensation of the nucleus and the enucleation process, and finally the maturation into erythrocytes.<sup>3,6</sup> Cells from late/terminal erythroid differentiation stages (erythroblast to erythrocytes) can easily be identified from other tissues with erythroid-specific cell-surface markers like glycoporphins.<sup>7</sup> In contrast, a unique cell-surface marker exclusive for intermediate erythroid differentiation stages around the proerythroblast stage has not been found so far.<sup>4</sup> Therefore, identification and isolation of these cells from other tissues and differentiation stages have been complex, as these methods required the use of multiple markers.<sup>8,9</sup> A unique cell-surface marker for intermediate erythroid differentiation stages would not only facilitate hematological research and diagnostics, but would enable the targeting of these cells for therapeutic purposes.

Parvovirus B19 (B19V) is a very small, nonenveloped virus, mainly known as the human pathogen causing the childhood

disease *erythema infectiosum*.<sup>10,11</sup> Productive viral infection of B19V is highly restricted to erythroid progenitor and precursor cells in the bone marrow. Susceptible cells are the erythroid differentiation stages from BFU-E to erythroblasts, where the proerythroblast stage represents the main target.<sup>12–14</sup> The glycosphingolipid globoside was found as a receptor for B19V,<sup>15</sup> serving as an attachment site for the virus on the cell surface.<sup>16</sup> However, the expression pattern of globoside and the proposed coreceptors  $\alpha 5 \beta 1$  integrin<sup>17</sup> or Ku80<sup>18</sup> cannot explain the extraordinary restricted internalization of B19V into erythroid progenitor and early precursor cells, suggesting a still unknown cellular receptor responsible for the virus uptake.<sup>19</sup>

We recently found that the unique region of the viral protein 1 (VP1u) mediates the targeting and specific uptake into these erythroid cells.<sup>20</sup> Furthermore, a C-terminal truncation ( $\Delta C126$ ) of the recombinant VP1u protein showed that the N-terminal 100 amino acids are sufficient for cell-specific internalization; in contrast, a short truncation from the N-terminus led to a dysfunctional protein ( $\Delta N30$ ) (Figure 1A).

This minimalistic and highly selective uptake mechanism encouraged us to design a viral-based delivery system that would maintain the specific cell-entry of the native virus and that would also allow the transport of versatile cargo into these cells. To address this issue, we conjugated the cell-targeting VP1u protein to NeutrAvidin as a loading platform for any biotinylated cargo molecules. This VP1u–NeutrAvidin complex served as a virus-like carrier for cellular delivery of biotinylated

Received: June 8, 2015

Revised: July 28, 2015

Published: August 4, 2015



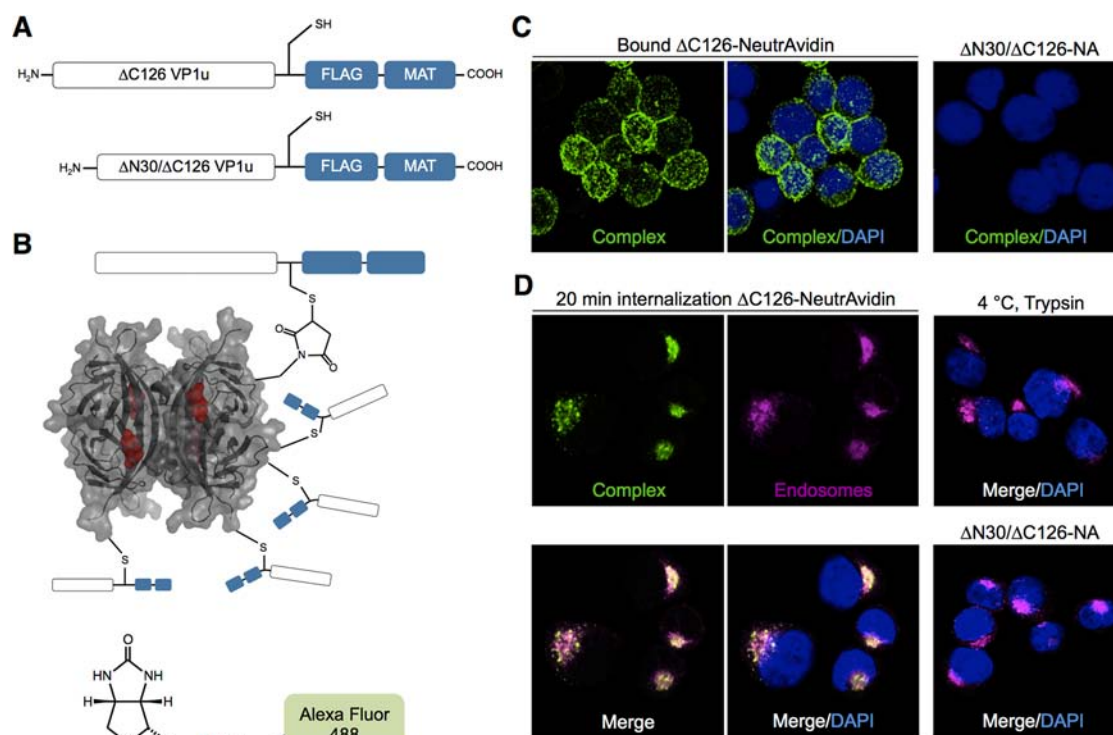


**Figure 1.** Endocytosis of the fluorescent VP1u–NeutrAvidin complex. (A) Schematic representation of the recombinant ΔC126 and ΔN30/ΔC126 VP1u of B19V with introduced unique cysteine and FLAG/MAT tag. (B) Model of the chemically engineered VP1u–NeutrAvidin complex (Avidin tetramer; gray; biotin binding sites; red). Detailed information in [SI Figure S1](#). (C) Representative images of VP1u–NeutrAvidin–AlexaFluor 488 complex (green) bound to erythroleukemic UT7/Epo cells at 4 °C: functional ΔC126 VP1u–NeutrAvidin (left) and dysfunctional ΔN30/ΔC126–NeutrAvidin control (right). (D) Internalization of ΔC126–NeutrAvidin–AlexaFluor 488 (left) and controls (right) at 37 °C. Endocytic pathway (early/late endosomes, lysosomes) was immunostained and shown in magenta. Fluorescence microscopy and imaging was performed with the Laser Scanning Microscope LSM 510 (63× magnification objective, Carl Zeiss).

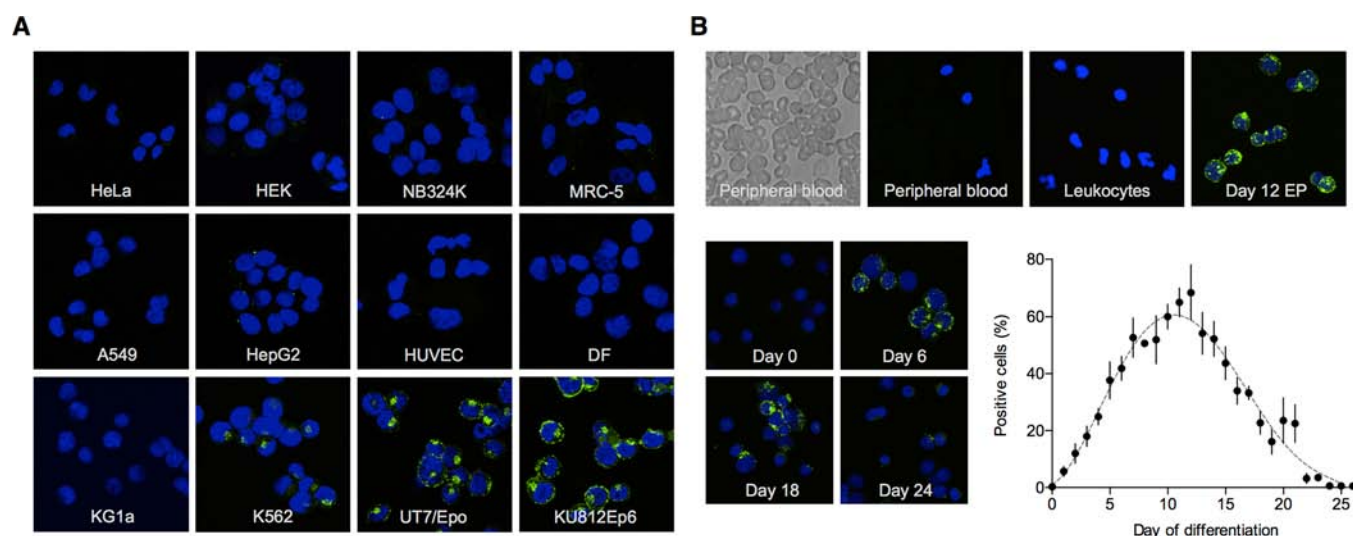


**Figure 2.** VP1u–NeutrAvidin specifically targets early erythroid precursors and erythroleukemic cells. ΔC126–NeutrAvidin–AlexaFluor 488 was incubated with different human cell types for 45 min at 37 °C. (A) Representative images of cells from different tissues (row 1 and 2) and hematopoietic cell lines (row 3; erythroleukemic types: K562, UT7/Epo, and KU812Ep6). (B) Representative images of primary hematopoietic cells: Peripheral blood cells and enriched leukocyte fraction; erythroid precursors (EP) originated from ex vivo expansion of CD34<sup>+</sup> stem cells with growth factors IL3, SCF, EPO, and hydrocortisone. VP1u–NeutrAvidin targeting along erythroid differentiation, shown by fluorescence microscopy images and plotted count of fluorescence-positive cells (three samples with  $n > 100$  cells).

cargo molecules. Our findings show that the VP1u–NeutrAvidin conjugate exclusively targets intermediate erythroid differentiation stages around the proerythroblast stage and

efficiently delivers fluorophores, DNA, and toxic payloads into this cell population.

## RESULTS

**VP1u–NeutrAvidin Complex Specifically Binds and Internalizes into Intermediate Erythroid Differentiation Stages.** To design the VP1u–NeutrAvidin conjugate, we introduced a unique cysteine into the recombinant  $\Delta$ C126 VP1u and thereby provided a sulfhydryl group for specific cross-linking chemistry (Figure 1A). The reduced VP1u was then coupled by Click Chemistry to maleimide-activated NeutrAvidin, resulting in about 5–6 covalently attached VP1u per NeutrAvidin tetramer (Figure 1B and SI Figure S1). The NeutrAvidin tetramer features 4 high affinity biotin binding sites, representing a docking platform for any biotinylated cargo molecule.

To test the internalization capability of the VP1u–NeutrAvidin construct, we used the fluorophore conjugate biotin–AlexaFluor 488 as a reporter cargo molecule. The green fluorescent complex was then incubated with erythroleukemic UT7/Epo cells for binding (4 °C) and uptake (37 °C). The dysfunctional N-terminal truncated VP1u ( $\Delta$ N30/ $\Delta$ C126) coupled to NeutrAvidin served as a negative control. The erythroleukemic UT7/Epo cell line is frequently used to study B19V entry, since these cells are similarly susceptible as the erythroid precursor cells in the bone marrow. In contrast to the erythroid precursor cells, UT7/Epo cells are only semi-permissive and do not support a productive viral amplification.<sup>21</sup>

The results indicate that the fluorescent VP1u–NeutrAvidin binds to UT7/Epo cells and then efficiently internalizes through the endocytic pathway, i.e., trafficking to early/late endosomes and finally to lysosomes (Figure 1C and D).

To examine the targeting specificity of the VP1u–NeutrAvidin complex, we tested the uptake of green fluorescent  $\Delta$ C126–NeutrAvidin on cell types from various tissues and hematopoietic lineages (Figure 2). The findings demonstrate that the VP1u–NeutrAvidin exclusively targets cells during a well-defined erythroid differentiation phase, including the erythroleukemic cell lines K562 (very low targeting), UT7/Epo, and KU812Ep6. To further define the VP1u–NeutrAvidin targeting along the erythroid differentiation, we expanded human CD34+ bone marrow stem cells *ex vivo* with the growth factors interleukin-3 (IL-3), stem cell factor (SCF), erythropoietin (EPO), and hydrocortisone toward the erythroid lineage. The erythroid development was assessed with established erythroid markers and differential morphology staining as previously described (SI Figure S2).<sup>22–24</sup> The results show that the binding and internalization of the fluorescent VP1u–NeutrAvidin strongly correlated with the intermediate erythroid differentiation stages from CFU-E to basophilic erythroblast.

These findings suggest that the EPO-dependent erythroid differentiation stages around the proerythroblastic/early basophilic stage are the main target of the VP1u–NeutrAvidin, which coincides with the tropism of the native virus.<sup>12–14,24</sup> To demonstrate the specificity of the fluorescent VP1u–NeutrAvidin conjugate as a marker for these intermediate erythroid differentiation stages, we generated samples with heterogeneous cell populations and tested for internalization of the conjugate in these cells. The results show that the fluorescent VP1u–NeutrAvidin specifically detects early erythroid precursors and erythroleukemic cell in heterogeneous cell populations like mixed cell cultures or peripheral blood (Figure 3G and SI Figure S3).

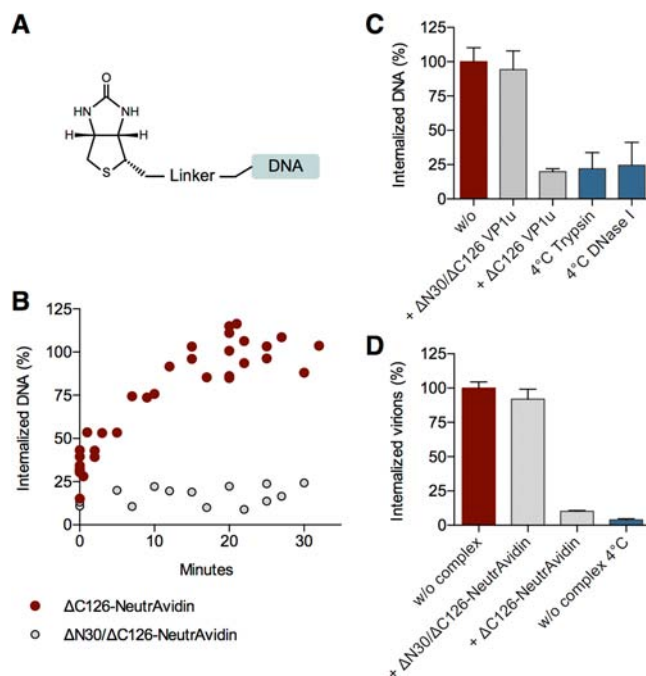


**Figure 3.** Delivery of DNA to erythroleukemic cells. (A) A biotin-PCR fragment (140 bp), amplified from the B19V genome, was coupled to VP1u–NeutrAvidin and incubated with UT7/Epo cells at 37 °C. The internalized DNA was extracted and detected by qPCR. (B) Quantitative uptake kinetics of  $\Delta$ C126–NeutrAvidin–DNA and  $\Delta$ N30/ $\Delta$ C126–NeutrAvidin–DNA. (C) Quantification of  $\Delta$ C126–NeutrAvidin–DNA uptake competed with excess of free VP1u variants (gray). Background of noninternalized complexes (4 °C) after treatment with trypsin or DNase I (blue). For all,  $n = 4$ . (D) Quantification of native B19V uptake in the presence of VP1u–NeutrAvidin ( $n = 4$ ). Values were normalized to unhindered internalization (dark red).

**VP1u–NeutrAvidin Delivers Oligonucleotides and Toxic Payloads to Erythroleukemic Cells.** In the native B19V, the VP1u has the crucial function to transport the capsid with the viral genome into the target cell. We wondered whether the VP1u–NeutrAvidin conjugate also features the capacity for DNA delivery. To address this question, we attached a biotinylated 140 bp PCR fragment (Figure 3A), amplified from the B19 viral genome, to the VP1u–NeutrAvidin and incubated this complex with UT7/Epo cells at 37 °C. After washes and trypsinization, the internalized DNA cargo was quantified by qPCR (Figure 3B). The observed kinetics indicate a rapid DNA uptake of more than 100 copies/cell and minute by the  $\Delta$ C126–NeutrAvidin complex, but not by the dysfunctional  $\Delta$ N30/ $\Delta$ C126–NeutrAvidin. Furthermore, the inhibition of the DNA internalization by excess of  $\Delta$ C126 VP1u confirmed that the uptake was mediated by the specific VP1u-targeting function (Figure 3C). As expected, the functional  $\Delta$ C126–NeutrAvidin complex strongly competed with B19V internalization, indicating a common uptake mechanism (Figure 3D).

Since erythroleukemias have proliferating cancer cells in the early and intermediate erythroid differentiation stages, we sought to use the VP1u–NeutrAvidin to specifically deliver toxins to these cells. To this end, we chose BSA as an adaptor carrier-molecule and used its 35 surface lysines<sup>25</sup> for Click Chemistry attachment of a single PEG-linked biotin and 20–30 lysosome-cleavable valine-citrulline monomethyl auristatin E



(VcMMAE) toxins<sup>26</sup> (Figure 4A and SI Figure S4). This toxic biotin-BSA was docked to VP1u–NeutrAvidin and applied to

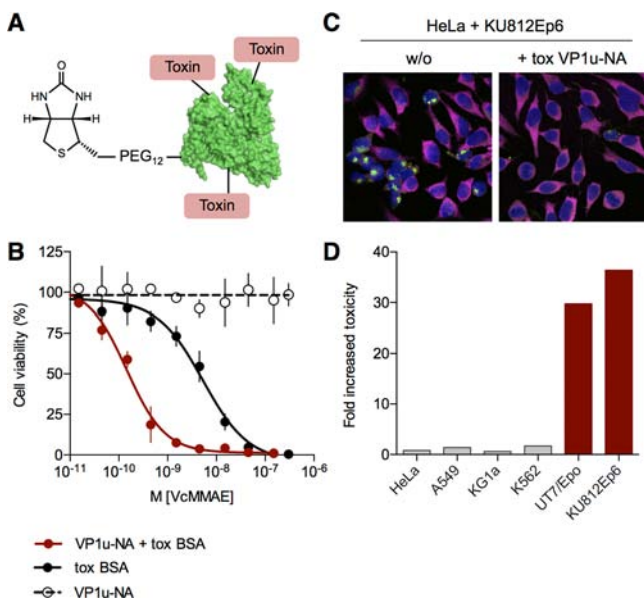


**Figure 4.** Delivery of toxic payloads to erythroleukemic cells. (A) Biotinylated and toxin-loaded BSA was coupled to VP1u–NeutrAvidin (VP1u–NA) and incubated with different cell lines. (B) Quantified cell viability of erythroid KU812Ep6 cells 5 days after incubation with different concentrations of the toxic VP1u–NeutrAvidin ( $n = 3$ ). (C) Representative pictures of the selective elimination of KU812Ep6 cells cocultured with HeLa cells by the toxic VP1u–NeutrAvidin (1 nM coupled VcMMAE, 5 days): GAPDH immunostained and shown in magenta,  $\Delta$ C126–NeutrAvidin–AlexaFluor 488 was added as marker for KU812Ep6 cells (green). (D) The calculated increase of the cell toxicity ( $IC_{50}$ ) mediated by specific VP1u–NeutrAvidin toxin delivery.

erythroleukemic KU812Ep6 cell cultures. Cell morphology as viability were monitored over a period of 5 days. After 2–3 h, the endocytosed VcMMAE toxin led to cell morphological changes typical of microtubule depolymerization. Toxic VP1u–NeutrAvidin-induced apoptosis and abnormal cell shapes were visible within 24 h postaddition, leading to low cell viability after 5 days (Figure 4B). In contrast, the background toxicity of the BSA-toxin without VP1u–NeutrAvidin was more than 30 times lower on KU812Ep6 cells. Targeted toxin delivery by the VP1u–NeutrAvidin was also observed on UT7/Epo cells (Figure 4D and SI Figure S6), correlating with the specificity for these erythroleukemic cells (Figure 2). Notably, the low targeting of K562 cells by the VP1u–NeutrAvidin did not lead to a significant decrease of the cell viability compared to the background toxicity.

The toxic monomethyl Auristatin E (MMAE) is released in the targeted cells by late endosomal and lysosomal cathepsin B, which specifically cleaves the valine-citrulline (Vc) dipeptide in the linker. The incubation of the biotin-BSA-fluorescein + VP1u–NeutrAvidin with different cell types for 90 min confirmed the accumulation of the complex in late endosomal and lysosomal compartments and exclusively in erythroleukemic cells (SI Figure S5). Correspondingly, the incubation of mixed cell populations with toxic VP1u–NeutrAvidin for 24 h specifically killed erythroleukemic cells without significant influence on other cells types (Figure 4C).

Importantly, the used maleimide-sulfhydryl Click Chemistry for the toxic VcMMAE attachment does not exhibit long-term

stability in cell culture medium due to sulfhydryl exchange with medium components.<sup>27</sup> To minimize such nonendosomal release of VcMMAE and thus unspecific toxicity, we exchanged the culture medium 24 h post-addition.

## DISCUSSION

Tissue-specific cell targeting is an important method in diagnostics and therapeutic applications. The targeting is typically performed by antibodies or receptor ligands, but viruses can also be used, especially for targeted gene and drug delivery. Despite extensive research, cells from intermediate erythroid differentiation stages such as proerythroblasts cannot be identified with a single cell-surface marker. The specific targeting of these cells would facilitate hematological diagnostics and would also enable the direct therapy of erythroid disorders like thalassemias or erythroleukemia. Here we report a viral-based targeting system that specifically detects cells around the proerythroblast stage and that can deliver cargo to these cells.

To generate this viral-based delivery system, we conjugated the VP1u of parvovirus B19 as a cell-specific viral targeting module to NeutrAvidin as a loading platform for biotinylated cargo. The advantage of NeutrAvidin as an adaptor platform increased the diversity for possible cargo molecules, since biotinylated compounds and biotinylation techniques are broadly available. Furthermore, the efficient and stable conjugation of a cargo to the cell-entering carrier is a critical step for the construction of a delivery system. For this purpose, the NeutrAvidin–biotin coupling represents a simple, versatile, and reliable approach, which can be performed within a wide range of temperature and buffers. Parvovirus B19 contains three VP1u per capsid<sup>28</sup> and thus might induce an efficient cellular uptake by a multivalent interaction. To mimic this viral property, we coupled multiple VP1u to one delivery platform, achieving about 5–6 VP1u per NeutrAvidin tetramer (SI Figure S1). In this context, the use of the same multivalent delivery system for the different cargos ensured similar uptake efficiency for each approach and thus enhanced the reliability of the overall method.

Using a biotinylated fluorescent dye as a reporter molecule, we demonstrated the specificity of the VP1u–NeutrAvidin for EPO-dependent erythroid differentiation stages around the proerythroblastic/early basophilic stage (Figure 2 and SI Figure S2). This restricted targeting profile coincides with that of the native B19 virus,<sup>12,14</sup> showing the fluorescent VP1u–NeutrAvidin as a reliable marker for B19V susceptible cells. These findings also indicate the VP1u-mediated uptake as a major determinant of the restricted B19 viral tropism. The previously proposed receptor globoside<sup>15</sup> and coreceptors  $\alpha 5 \beta 1$  integrin<sup>17</sup> and Ku80<sup>18</sup> might be involved in certain binding steps of the virus, but their broad expression pattern cannot explain the highly restricted cellular uptake and narrow tropism of B19V. The discrepancy between receptor expression and actual B19V internalization has often led to confusion regarding which cell types are susceptible to B19V. In this context, the fluorescent VP1u–NeutrAvidin is a specific marker that will help to clarify which cells allow internalization of the native virus. The definition of the susceptible cell types is essential to understand the pathogenesis of B19V infection and its associated disorders.

In addition to the VP1u-mediated internalization, an antibody-dependent uptake of B19V into endothelial cells has been reported.<sup>29,30</sup> Importantly, this antibody-dependent entry

represents a late viremic phase phenomenon and furthermore does not lead to a productive viral replication. Nevertheless, the binding and internalization of these immune complexes on the endothelial tissues and immune cells can explain inflammatory manifestations during B19V infection.<sup>29,30</sup>

The unique targeting profile of the VP1u raises the intriguing possibility of a yet unknown cellular receptor exclusively expressed during the intermediate erythroid differentiation and which is not found on other tissues and tested cell types.<sup>3,4,8,9,31,32</sup> It will be important to identify this structure and to elucidate its physiological role in erythropoiesis.

To date, the identification and isolation of intermediate erythroid differentiated cells from other tissues and other differentiation stages have been difficult, since the currently used markers are not lineage-specific (CD71, CD36, CD38, CD45, CD105, EPOR) or are broadly expressed during the erythroid development (glycophorin A).<sup>3,4,8,9,31–33</sup> Therefore, the combination of several markers is necessary to identify these erythroid differentiation stages, which is rather complex and laborious. In contrast, the fluorescent VP1u–NeutrAvidin appeared as a unique marker for intermediate erythroid differentiation stages (Figure 2) and specifically detected early erythroid precursors or erythroleukemic cells in heterogeneous cell populations from different tissues (Figure 3G and SI Figure S3). This result shows the potential of the fluorescent VP1u–NeutrAvidin as a marker in hematological research and diagnostics. As a specific example, diverse hematological disorders like leukemia, thalassemia, or the myelodysplastic syndrome are typically associated with the presence of erythroblasts outside the bone marrow.<sup>3,34</sup> The fluorescent VP1u–NeutrAvidin can specifically detect early erythroid precursors in the peripheral blood (SI Figure S3) and can therefore be used as a sensitive marker for the early identification of such hematological disorders.

Many erythroid disorders are caused by genetic defects resulting in aberrant or incorrect expression of erythroid proteins. A gene therapy approach of these disorders would require a gene or antisense delivery before or during the protein expression. Erythroid-specific proteins are typically expressed during the intermediate and terminal erythroid differentiation stages; however, a specific targeting and delivery to these cells is currently not feasible. As a representative example, a significant proportion of thalassemias is caused by splicing errors of the globin pre-mRNA. As previously shown, the delivery of antisense oligonucleotides into globin expressing cells can restore this aberrant splicing.<sup>35,36</sup> Our results show that the VP1u–NeutrAvidin delivers short DNA fragments specifically into intermediate erythroid differentiations stages, in which the expression and accumulation of erythroid specific proteins begins. This selective targeting and delivery of nucleic acids provides a novel approach for erythroid specific gene therapies.

Acute erythroleukemia is a rare disorder associated with a poor prognosis. The treatment of erythroleukemia is compromised due to the systemic distribution and resistance of the malignant cells to chemotherapeutics.<sup>5,37</sup> Therefore, the successful elimination of erythroleukemic cells by a cytotoxin requires a 'magic bullet' strategy, an efficient and specific targeting of the toxin to cancer cells, preventing harmful effects to the surrounding healthy tissue.<sup>38</sup> Since erythroleukemias have proliferating cancer cells in the early and intermediate erythroid differentiation stages, we sought to use the VP1u–NeutrAvidin to deliver toxins to these cells. The results showed that the VP1u–NeutrAvidin targeted toxin specifically to

malignant erythroid precursors and thus selectively eliminated these cells from a mixed cell culture (Figure 4C). In conclusion, the VP1u-mediated toxin delivery represents a promising strategy to overcome the resistance of erythroleukemia to chemotherapeutics.

Taken together, we report a viral-based delivery system that features the B19 viral properties as a specific carrier to early erythroid precursors around the proerythroblast stage. The unique targeting of these intermediate erythroid differentiations stages offers new opportunities for hematological diagnostics and therapeutic applications.

## MATERIALS AND METHODS

**Cells.** Cell lines were obtained from ATCC if not indicated otherwise and cultured at 37 °C, 5% CO<sub>2</sub>. UT7/Epo cells were kindly provided by E. Morita (Tohoku University School of Medicine, Japan) and grown in RPMI 1640, 5% fetal calf serum (FCS), 2 U/mL recombinant human erythropoietin (rhEPO). KU812Ep6 cells were kindly provided by N. Ikeda (Fujire-bio, Inc., Tokyo, Japan) and cultured in RPMI 1640, 5% FCS, 6 U/mL rhEPO. Primary human fibroblasts were cultured in provided fibroblast basal medium with fibroblast growth kit components (ATCC). Similarly, primary HUVEC cells were cultured in F-12K medium with endothelial cell growth supplements. The other cell lines were cultured as follows: K562 in IMDM 5% FCS; KG1a in IMDM 20% FCS; HepG2 in MEM/EBSS 5% FCS; HeLa, HEK 293T, NB324 K, MRC-5, and A549 all in DMEM 5% FCS. Culture media for cell lines were all supplemented with penicillin/streptomycin and L-alanyl-L-glutamine. Peripheral blood was obtained from a blood transfusion service (BSD SRK, Bern, Switzerland). To enrich the leukocyte fraction, we treated peripheral blood cells with red blood cell lysis buffer (155 mM NH<sub>4</sub>Cl, 12 mM NaHCO<sub>3</sub>, 0.1 mM EDTA) and washed three times (250 g). CD34+ stem cells (Stemcell Technologies, Grenoble, France) were expanded in serum-free media according to a previously described one phase protocol.<sup>22–24</sup> Cells were cultured in  $\alpha$ MEM medium supplemented with 20% BIT 9500 (BSA, insulin, transferrin), 90 ng/mL ferric nitrate, 900 ng/mL ferrous sulfate, 100 ng/mL stem cell factor (SCF), 5 ng/mL interleukin 3 (IL-3), 1  $\mu$ M hydrocortisone, and 3 U/mL rhEPO to induce differentiation toward the erythroid lineage. Erythroid differentiation was confirmed with the erythroid markers transferrin receptor, glycophorin A, glycophorin C, and Wright-Giemsa stain (SI Figure S2).

**Antibodies.** Mouse mAb against early endosomes (70521; anti-EEA1), late endosomes (2733 2G11; anti-mannose 6 phosphate receptor [M6PR]), lysosomes (H4A3; anti-LAMP1), glycophorin A (HIR2), glycophorin C (E5), and anti-GAPDH (6C5) were obtained from Abcam (Cambridge, MA). Human fluorescein-labeled transferrin was purchased from Exbio (Vestec, Czech Republic).

**Coupling Reagents.** Maleimide-activated NeutrAvidin, biotin-PEG<sub>12</sub>-N-hydroxysuccinimide (NHS) ester and maleimide-fluorescein were obtained from Thermo Scientific (Waltham, MA). Biocytin-Alexa Fluor 488 was obtained from Life Technologies (Carlsbad, CA). Bovine serum albumin (BSA) and 3-(2-pyridyldithio)propionic acid NHS ester were purchased from Sigma (St. Louis, MO). Maleimide valine-citrulline monomethyl auristatin E (VcMMAE) was obtained from MedChem Express (Princeton, NJ).

**VP1u Cloning and Expression.** Generation of recombinant VP1u was performed as previously described.<sup>20</sup> The VP1u

sequence originally derived from the infectious clone pB19-M20 (S. Wong, National Institutes of Health, Bethesda, MD) and was cloned into the pT7-FLAG-MAT-Tag-2 expression vector (Sigma). Truncations ( $\Delta$ C126 and  $\Delta$ N30) were introduced by QuikChange PCR (Agilent Technologies, Santa Clara, CA) and corresponding deletion primers as previously described.<sup>20</sup> Protein expression in BL21(DE3) *E. coli* was induced with 1 mM isopropyl- $\beta$ -D-thiogalactopyranoside (IPTG) at an optical density ( $OD_{600}$ ) of 0.6 for 4 h and 37 °C. Recombinant VP1u was purified twice with Ni-NTA agarose under native conditions according to the manufacturer's protocol (Qiagen, Venlo, Netherlands) (SI Figure S1).

**VP1u–NeutrAvidin Coupling and Purification.** Sulfhydryl to maleimide Click Chemistry reactions were carried out in neutral phosphate buffer saline (PBS, pH 6.5–7.5) and under reducing conditions with tris(2-carboxyethyl)-phosphine (TCEP). Recombinant VP1u in reducing PBS (50 mM  $NaH_2PO_4$ , 150 mM NaCl, 5 mM TCEP, pH 7) was added to maleimide-activated NeutrAvidin, resuspended in PBS (pH 7) + 10% glycerol. Cross-linking was allowed for 6 h at room temperature and overnight at 4 °C. VP1u–NeutrAvidin conjugates were purified twice with Ni-NTA agarose and once with iminobiotin agarose (Thermo Scientific) to remove unreacted components. The construct was passed through a PBS equilibrated PD-10 desalting column (GE Healthcare, Chalfont St. Giles, GB) to remove the elution buffer and column remnants. Coupling efficiency and purity were examined by SDS-PAGE (SI Figure S1).

**Green Fluorescent VP1u–NeutrAvidin.** To generate the green fluorescent VP1u–NeutrAvidin, we incubated the VP1u–NeutrAvidin complexes with a 4-fold molecular excess of biocytin-Alexa Fluor 488 for 1 h at 4 °C in PBS + 1% BSA (PBSA). Fluorescent complexes ( $3 \times 10^{12}$ ) were then added to cells ( $3 \times 10^5$ ) in 100  $\mu$ L culture medium. Binding was performed at 4 °C for 1 h and four subsequent washes with ice-cold PBS (Figure 1C); internalization was carried out for 20 min at 37 °C with two subsequent washes, trypsinization, and further two washes (Figure 1D). Fluorescent VP1u–NeutrAvidin targeting to different cell types (Figure 2) was examined by incubation of fluorescent complex with cells for 45 min at 37 °C and subsequent four washes without trypsinization. Cells were fixed with ice-cold acetone/methanol (1:1) and immunostained if required. Fluorescent signal was detected with the Laser Scanning Microscope LSM 510 (63 $\times$  magnification objective, Carl Zeiss) and images were further processed with BioImageXD.<sup>39</sup>

**VP1u–NeutrAvidin–DNA.** 5'-Biotinylated DNA fragment (140 bp) was produced by PCR amplification from B19 viral genome with following primers: forward biotin-5'-GGGC-AGCCATTTTAAGTGTTT-3' and reverse 5'-CCAGGAA-AAAGCAGCCCAG-3'. DNA fragments ( $4 \times 10^{11}$ ) were coupled with VP1u–NeutrAvidin constructs ( $10^{11}$ ) and then added to UT7/Epo cells ( $5 \times 10^5$ ) in 100  $\mu$ L culture medium. Standard internalization was carried out for 20 min at 37 °C with subsequent two washes/trypsinization/two washes. DNase I (25 units, Roche) was tested as alternative to trypsin treatment, resulting in similar removal of noninternalized DNA fragments as trypsinization (Figure 3C). VP1u–NeutrAvidin–DNA uptake was competed with 400 ng ( $2 \times 10^{13}$ ) free VP1u molecules. For competition of native B19V uptake by excess VP1u–NeutrAvidin, UT7/Epo cells were incubated with human B19V infected plasma containing  $3 \times 10^{10}$  virions in the presence of  $3 \times 10^{12}$  VP1u–NeutrAvidin molecules (Figure

3D). Cell-internalized DNA was extracted with the DNeasy Blood and Tissue Kit (Qiagen) and quantified by iTaq SybrGreen qPCR (BioRad, Hercules, CA; primers: forward 5'-GGGCAGCCATTTTAAGTGTTT-3', reverse 5'-CCA-GGAAAAAGCAGCCCAG-3'. A B19 virus infected plasma sample was obtained from our donation center<sup>40</sup> (genotype 1) (CSL Behring AG, Charlotte, NC).

**Toxic VP1u–NeutrAvidin.** BSA (10 mg/mL) in PBS (pH 7.4) was incubated with a 1.1-fold molecular excess (1.1 $\times$ ) of biotin-PEG<sub>12</sub>-NHS ester for 2 h at 30 °C to achieve cross-linking of  $\sim$ 1 biotin/BSA (SI Figure S4). This product was further incubated with a 100-fold molecular excess 3-(2-pyridyldithio)propionic acid NHS ester (4 h, 30 °C) to achieve transformation of primary amines on BSA surface to lysine–S–S-pyridyl groups. Coupled product was purified by size exclusion (Zeba plates, 40 kDa MWCO; Thermo Scientific) and disulfide bonds were subsequently reduced by TCEP (50 mM  $NaH_2PO_4$ , 150 mM NaCl, 5 mM TCEP, pH 7). Free sulfhydryl groups were coupled by Click Chemistry with maleimide–VcMMAE or maleimide–fluorescein (maleimide/sulfhydryl ratio 5:1). Coupling was allowed for 6 h at 30 °C and labeled BSA was then purified by size exclusion (Zeba plates, 40 kDa MWCO). Coupling efficiency was analyzed by SDS-PAGE (SI Figure S4), indicating 20–30 attached VcMMAE or fluorescein molecules per BSA protein (biotin<sub>1</sub>-BSA-VcMMAE<sub>20–30</sub> and biotin<sub>1</sub>-BSA-fluorescein<sub>20–30</sub>, respectively).

To produce toxic VP1u–NeutrAvidin, we incubated biotin<sub>1</sub>-BSA-VcMMAE<sub>20–30</sub> with VP1u–NeutrAvidin (ratio 2:1) in PBSA for 1 h at room temperature. VP1u–NeutrAvidin-toxicBSA<sub>2</sub> complex (toxic VP1u–NeutrAvidin) was then added at different concentrations to  $5 \times 10^3$  seeded cells in a 96-well plate. Culture medium was exchanged 24 h later to minimize unspecific effects due to nonendosomal toxin release. Cells were then further cultured in fresh medium and viability was quantified after 5 days with AlamarBlue reagent (Life Technologies), using a fluorescence plate reader (Infinite M1000 PRO, Tecan).

**Statistics from Quantitative Methods.** Values are shown as means  $\pm$  standard deviation. Replicates represent values from independent experiments. Cell count of fluorescence-positive erythroid cells in Figure 2B was performed by trained personnel. Cells were rated as 'negative' (value = 0), 'weak positive' (= 0.5), and 'positive' (= 1). Plotted values indicate the average percentage and standard deviation from three samples (each  $n > 100$ ).

## ■ ASSOCIATED CONTENT

### § Supporting Information

The Supporting Information is available free of charge on the ACS Publications website at DOI: 10.1021/acs.bioconjchem.5b00321.

Supplemental figures of VP1u–NeutrAvidin SDS PAGE, ex vivo erythroid differentiation, detection of erythroid precursors in peripheral blood, BSA modifications, fluorescein-BSA delivery, and IC<sub>50</sub> of toxin delivery (PDF)

## ■ AUTHOR INFORMATION

### Corresponding Authors

\*E-mail: remo.leisi@dcb.unibe.ch.

\*E-mail: carlos.ros@ibc.unibe.ch. Phone: +41 31 631 43 49.

Fax: +41 31 631 48 87.



## Author Contributions

R.L. conceived the study, designed and performed experiments, analyzed data, drafted and wrote the manuscript. M.V.N. designed and performed experiments, collected data, and corrected the manuscript. C.K. and C.R. conceived the study, provided expert consultation, drafted and revised the manuscript.

## Notes

The authors declare no competing financial interests.

## REFERENCES

- (1) An, X., Schulz, V. P., Li, J., Wu, K., Liu, J., Xue, F., Hu, J., Mohandas, N., and Gallagher, P. G. (2014) Global transcriptome analyses of human and murine terminal erythroid differentiation. *Blood* 123, 3466–77.
- (2) Richmond, T. D., Chohan, M., and Barber, D. L. (2005) Turning cells red: signal transduction mediated by erythropoietin. *Trends Cell Biol.* 15, 146–55.
- (3) Koury, M. J. (2014) Abnormal erythropoiesis and the pathophysiology of chronic anemia. *Blood Rev.* 28, 49–66.
- (4) Machherndl-Spandl, S., Suessner, S., Danzer, M., Proell, J., Gabriel, C., Lauf, J., Sylke, R., Klein, H. U., Bene, M. C., Weltermann, A., et al. (2013) Molecular pathways of early CD105-positive erythroid cells as compared with CD34-positive common precursor cells by flow cytometric cell-sorting and gene expression profiling. *Blood Cancer J.* 3, e100.
- (5) Wickrema, A., and Crispino, J. D. (2007) Erythroid and megakaryocytic transformation. *Oncogene* 26, 6803–15.
- (6) Loken, M. R., Shah, V. O., Dattilio, K. L., and Civin, C. I. (1987) Flow cytometric analysis of human bone marrow: I. Normal erythroid development. *Blood* 69, 255–63.
- (7) Della Porta, M. G., Malcovati, L., Invernizzi, R., Travaglino, E., Pascutto, C., Maffioli, M., Galli, A., Boggi, S., Pietra, D., Vanelli, L., et al. (2006) Flow cytometry evaluation of erythroid dysplasia in patients with myelodysplastic syndrome. *Leukemia* 20, 549–55.
- (8) Chen, K., Liu, J., Heck, S., Chasis, J. A., An, X., and Mohandas, N. (2009) Resolving the distinct stages in erythroid differentiation based on dynamic changes in membrane protein expression during erythropoiesis. *Proc. Natl. Acad. Sci. U. S. A.* 106, 17413–8.
- (9) Hu, J., Liu, J., Xue, F., Halverson, G., Reid, M., Guo, A., Chen, L., Raza, A., Galili, N., Jaffray, J., et al. (2013) Isolation and functional characterization of human erythroblasts at distinct stages: implications for understanding of normal and disordered erythropoiesis in vivo. *Blood* 121, 3246–53.
- (10) Young, N. S., and Brown, K. E. (2004) Parvovirus B19. *N. Engl. J. Med.* 350, 586–97.
- (11) Heegaard, E. D., and Brown, K. E. (2002) Human parvovirus B19. *Clin. Microbiol. Rev.* 15, 485–505.
- (12) Ozawa, K., Kurtzman, G., and Young, N. (1986) Replication of the B19 parvovirus in human bone marrow cell cultures. *Science* 233, 883–6.
- (13) Ozawa, K., Kurtzman, G., and Young, N. (1987) Productive infection by B19 parvovirus of human erythroid bone marrow cells in vitro. *Blood* 70, 384–91.
- (14) Takahashi, T., Ozawa, K., Takahashi, K., Asano, S., and Takaku, F. (1990) Susceptibility of human erythropoietic cells to B19 parvovirus in vitro increases with differentiation. *Blood* 75, 603–10.
- (15) Brown, K. E., Anderson, S. M., and Young, N. S. (1993) Erythrocyte P antigen: cellular receptor for B19 parvovirus. *Science* 262, 114–7.
- (16) Nasir, W., Nilsson, J., Olofsson, S., Bally, M., and Rydell, G. E. (2014) Parvovirus B19VLP recognizes globoside in supported lipid bilayers. *Virology* 456–457, 364–9.
- (17) Weigel-Kelley, K. A., Yoder, M. C., and Srivastava, A. (2003) Alpha5beta1 integrin as a cellular coreceptor for human parvovirus B19: requirement of functional activation of beta1 integrin for viral entry. *Blood* 102, 3927–33.
- (18) Munakata, Y., Saito-Ito, T., Kumura-Ishii, K., Huang, J., Kodera, T., Ishii, T., Hirabayashi, Y., Koyanagi, Y., and Sasaki, T. (2005) Ku80 autoantigen as a cellular coreceptor for human parvovirus B19 infection. *Blood* 106, 3449–56.
- (19) Chen, A. Y., Guan, W., Lou, S., Liu, Z., Kleiboeker, S., and Qiu, J. (2010) Role of erythropoietin receptor signaling in parvovirus B19 replication in human erythroid progenitor cells. *J. Virol.* 84, 12385–96.
- (20) Leisi, R., Ruprecht, N., Kempf, C., and Ros, C. (2013) Parvovirus B19 uptake is a highly selective process controlled by VP1u: a novel determinant of viral tropism. *J. Virol.* 87, 13161–13167.
- (21) Wolfisberg, R., Ruprecht, N., Kempf, C., and Ros, C. (2013) Impaired genome encapsidation restricts the in vitro propagation of human parvovirus B19. *J. Virol. Methods* 193, 215–25.
- (22) Panzenbock, B., Bartunek, P., Mapara, M. Y., and Zenke, M. (1998) Growth and differentiation of human stem cell factor/erythropoietin-dependent erythroid progenitor cells in vitro. *Blood* 92, 3658–68.
- (23) von Lindern, M., Zauner, W., Mellitzer, G., Steinlein, P., Fritsch, G., Huber, K., Lowenberg, B., and Beug, H. (1999) The glucocorticoid receptor cooperates with the erythropoietin receptor and c-Kit to enhance and sustain proliferation of erythroid progenitors in vitro. *Blood* 94, 550–9.
- (24) Wong, S., Zhi, N., Filippone, C., Keyvanfar, K., Kajigaya, S., Brown, K. E., and Young, N. S. (2008) Ex vivo-generated CD36+ erythroid progenitors are highly permissive to human parvovirus B19 replication. *J. Virol.* 82, 2470–6.
- (25) Hermanson, G. (2008) *Bioconjugation techniques*, 2nd ed., Academic Press, New York.
- (26) Doronina, S. O., Toki, B. E., Torgov, M. Y., Mendelsohn, B. A., Cervený, C. G., Chace, D. F., DeBlanc, R. L., Gearing, R. P., Bovee, T. D., Siegall, C. B., et al. (2003) Development of potent monoclonal antibody auristatin conjugates for cancer therapy. *Nat. Biotechnol.* 21, 778–84.
- (27) Shen, B. Q., Xu, K., Liu, L., Raab, H., Bhakta, S., Kenrick, M., Parsons-Reponte, K. L., Tien, J., Yu, S. F., Mai, E., et al. (2012) Conjugation site modulates the in vivo stability and therapeutic activity of antibody-drug conjugates. *Nat. Biotechnol.* 30, 184–9.
- (28) Cotmore, S. F., McKie, V. C., Anderson, L. J., Astell, C. R., and Tattersall, P. (1986) Identification of the major structural and nonstructural proteins encoded by human parvovirus B19 and mapping of their genes by procaryotic expression of isolated genomic fragments. *J. Virol.* 60, 548–57.
- (29) von Kietzell, K., Pozzuto, T., Heilbronn, R., Grossl, T., Fechner, H., and Weger, S. (2014) Antibody-mediated enhancement of parvovirus B19 uptake into endothelial cells mediated by a receptor for complement factor C1q. *J. Virol.* 88, 8102–15.
- (30) Munakata, Y., Kato, I., Saito, T., Kodera, T., Ishii, K. K., and Sasaki, T. (2006) Human parvovirus B19 infection of monocytic cell line U937 and antibody-dependent enhancement. *Virology* 345, 251–7.
- (31) Spivak, J. L. (2005) The anaemia of cancer: death by a thousand cuts. *Nat. Rev. Cancer* 5, 543–55.
- (32) Anagnostou, A., Liu, Z., Steiner, M., Chin, K., Lee, E. S., Kessimian, N., and Noguchi, C. T. (1994) Erythropoietin receptor mRNA expression in human endothelial cells. *Proc. Natl. Acad. Sci. U. S. A.* 91, 3974–8.
- (33) Jelkmann, W., Bohlius, J., Hallek, M., and Sytkowski, A. J. (2008) The erythropoietin receptor in normal and cancer tissues. *Crit. Rev. Oncol. Hematol.* 67, 39–61.
- (34) Buttarello, M., and Plebani, M. (2008) Automated blood cell counts: state of the art. *Am. J. Clin. Pathol.* 130, 104–16.
- (35) Xu, J., Peng, C., Sankaran, V. G., Shao, Z., Esrick, E. B., Chong, B. G., Ippolito, G. C., Fujiwara, Y., Ebert, B. L., Tucker, P. W., et al. (2011) Correction of sickle cell disease in adult mice by interference with fetal hemoglobin silencing. *Science* 334, 993–6.
- (36) Suwanmanee, T., Sierakowska, H., Fucharoen, S., and Kole, R. (2002) Repair of a splicing defect in erythroid cells from patients with beta-thalassemia/HbE disorder. *Mol. Ther.* 6, 718–26.

- (37) Mazzella, F. M., Kowal-Vern, A., Shrit, M. A., Rector, J. T., Cotelingam, J. D., and Schumacher, H. R. (2000) Effects of multidrug resistance gene expression in acute erythroleukemia. *Mod. Pathol.* 13, 407–13.
- (38) Schwartz, R. S. (2004) Paul Ehrlich's magic bullets. *N. Engl. J. Med.* 350, 1079–80.
- (39) Kankaanpää, P., Paavolainen, L., Tiitta, S., Karjalainen, M., Paivarinne, J., Nieminen, J., Marjomäki, V., Heino, J., and White, D. J. (2012) BioImageXD: an open, general-purpose and high-throughput image-processing platform. *Nat. Methods* 9, 683–9.
- (40) Bonsch, C., Zuercher, C., Lieby, P., Kempf, C., and Ros, C. (2010) The globoside receptor triggers structural changes in the B19 virus capsid that facilitate virus internalization. *J. Virol.* 84, 11737–46.